analytical chemistry

Article

pubs.acs.org/ac

Molecular Hydrogel-Stabilized Enzyme with Facilitated Electron Transfer for Determination of H_2O_2 Released from Live Cells

Jie Zhou, Chuanan Liao, Limin Zhang, Qigang Wang,* and Yang Tian*

Department of Chemistry, Tongji University, Siping Road 1239, Shanghai 200092, P. R. China

Supporting Information

ABSTRACT: In this work, small molecular hydrogel was first employed as a surrounding matrix to stabilize an enzyme model, Cytochrome c (Cyt c), and more importantly to facilitate electron transfer between redox enzyme and electrode. Direct electron transfer of Cyt c was successfully achieved in the molecular hydrogel with redox formal potential ($E^{0\prime}$) of 100.7 ± 3.2 mV versus AglAgCl and heterogeneous electron transfer rate constant (k_s) up to 18.6 ± 2.3 s^{-1}. Experimental data demonstrated that Cyt c was stably immobilized into the molecular hydrogel and retained its inherent bioactive activity toward H_2O_2. The direct redox reaction of Cyt c, followed by the biochemical reaction between Cyt c and H_2O_2, established a reliable approach to determine H_2O_2 at an optimized potential with high selectivity over other reactive oxygen species (ROS), oxygen, metal ions, ascobic acid (AA), and so on. In addition, the present biosensor for H_2O_2 also exhibited wide linear range and low detection limit, which fulfills the requirements for detection of H_2O_2 in a biological system. The remarkable analytical performance of the present biosensor, as well as the long-term stability and good reproducibility ascribed to the molecular hydrogel-stabilized enzyme, provided a durable platform for real-time determination of H_2O_2 from live cells.

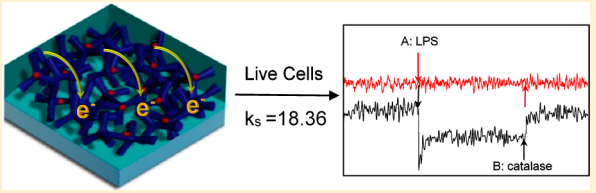

Direct electron transfer of enzymes and proteins plays an essential role, not only in physiological and pathological events but also in the determination of biochemical species by transduction into an electrical signal in biosensors or into electrical current in biofuel cells.[1−3] Therefore, the routing of electrons from redox enzymes to electron conductors (i.e., electrodes) is the subject of extensive research. A burst of research activity has focused on the modification of electrodes or enzymes themselves for creating accessible electron transfer interfaces, because direct contact between redox enzymes and metal electrode surfaces usually leads to significant structural and/or functional changes of enzymes.[4−6] On the basis of direct electrochemical redox reaction of enzyme, the third generation biosensor is proposed. Cytochrome c (Cyt c) is an excellent model for studying the electron transfer of typical enzymes from a structure point of view.[7,8] In addition, for further applications, it is easy for a Cyt c-based biosensor to avoid the interference from O_2 under an optimized working potential, since Cyt c is not a specific protein for O_2, unlike hemoglobin and myoglobin which are the carriers of O_2 in a biological system. In the past couple of decades, numerous approaches of chemically or nonchemically modified methods to the direct electron transfer of Cyt c have been exploited.[9−11] Our group is also very interested in electron transfer of Cyt c and has systematically investigated redox kinetics of Cyt c at various electrode surfaces, such as gold nanostructures, TiO_2 nanoparticles and nanoneedles, ZnO nanosheets, and Au-TiO_2 nanocomposites.[12−17] On the basis of the direct electron transfer of Cyt c, the developed biosensors for H_2O_2 have demonstrated high selectivity, good sensitivity, and wide detection linear range. Generally, the immobilization of Cyt c in designed biocompatible structures can siginificantly facilitate its electron transfer and improve the performance of biocatalytic processes.

Recently, molecular hydrogels, formed by self-assembly of small amphiphilic molecules, have attracted tremendous scientific and technological attention because they serve as scaffolds for tissue engineering, medium for screening inhibitors of enzymes, biomaterials for wound healing, and so on.[18−20] Hamachi and his group reported that supramolecular hydrogel can preserve the active sites of enzymes and serve as a transportable scaffold for biological activity.[21] Xu and his group found that the enzymes enclosed within peptide-based molecular hydrogels even exhibited apparent "superactivity" due to their hydrophilic nature in the network.[22,23] They also reported that the enzymes enclosed in the molecular hygrogels exhibited higher bioactivity up to eight times.[24] The promising results motivitated us to develop molecular hydrogels as new electrode materials and immobilize Cyt c into the three-dimensional (3D) hydrogels with high biocompatibility for facilitating electron transfer of Cyt c and enhancing the biocatalytic performance of Cyt c-based biosensors. Although conducting polymer hydrogels and aerogels have been widely employed as electrode materials for glucose sensors, capacitors, and so on,[25−29] to the best of our knowledge, few papers have been reported in which molecular hydrogels are employed for

Received: January 18, 2014
Accepted: April 10, 2014
Published: April 10, 2014

   dx.doi.org/10.1021/ac500231e | *Anal. Chem.* 2014, 86, 4395−4401

Scheme 1. Schematic Illustration for the Preparation Processes of Cyt c/Gel/ITO Electrode

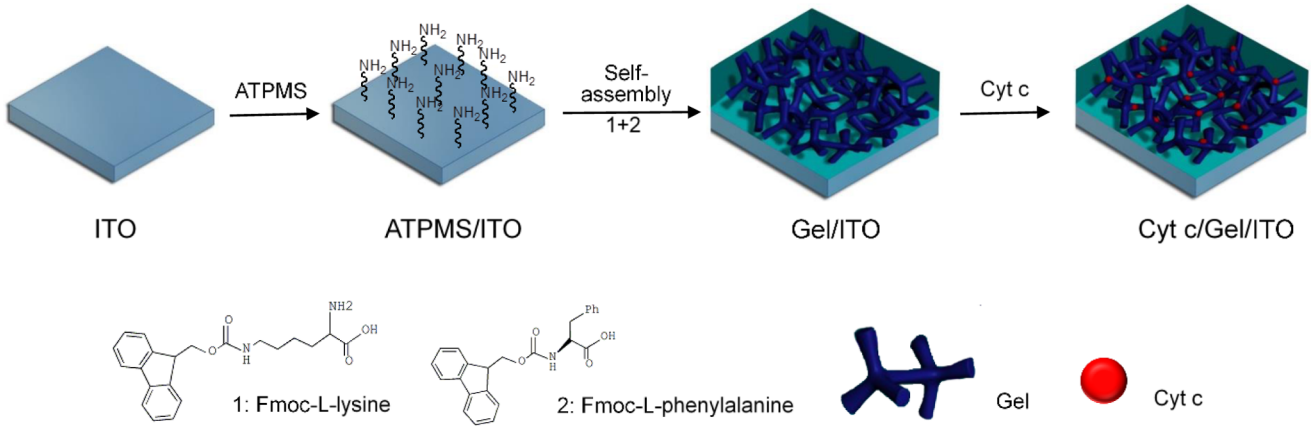

faciliting electron transfer of enzymes and constructing third-generation biosensors.

In the present work, direct electron transfer of Cyt c was first exploited in small molecular hydrogels with a formal potential of 100.7 ± 3.2 mV versus AglAgCl, which was formed at an ITO electrode surface by self-assembly of two simple derivatives of amino acids. We found that the redox reaction of Cyt c was greatly enhanced when it was enclosed in the molecular hydrogels with heterogenrous electron transfer rate constant (k_s) up to 18.6 ± 2.3 s^{-1}. Electrochemical and spectroscopic results indicated that Cyt c was immobilized in the 3D hydrogels with long-term stability and maintained its high enzymatic activity toward H_2O_2. A combination of direct electrochemistry and high bioelectrocatalytic activity of Cyt c in the molecular hydrogels paved a way for constructing a third-generation biosensor of H_2O_2 with enhanced analytical performance.[30] The present H_2O_2 biosensor showed high selectivity against typical reactive oxygen species such as $O_2^{\bullet-}$, $ROO^{\bullet}$, ClO^-, NO, and HNO; metal ions including Na^+, K^+, Ca^{2+}, Mg^{2+}, Mn^{2+}, Pb^{2+}, Co^{2+}, Cd^{2+}, Ni^{2+}, Zn^{2+}, Ag^+, Fe^{2+}, and Fe^{3+}; and other biological species such as uric acid (UA), ascobic acid (AA), dopamine (DA), and so on. Besides this, a good detection linear range was obtained from 3×10^{-7} to 8×10^{-4} M with a detection limit of 50 nM. More interestingly, the 3D scaffold of molecular hydrogels provided the immoblization of Cyt c with long-term stability up to 2 weeks and good reproducibility. These remarkable analytical performances, together with the biocompatibility of molecular hydrogels themselves, estabilished a reliable and durable approach to determine the H_2O_2 released from liver cancer cells.

EXPERIMENTAL SECTION

Reagents and Chemicals. Indium tin oxide (ITO)-coated glass plates with a square resistance of ~10 Ω cm^{-2} were purchased from Nanbo Display Technology Co. Ltd. (Shenzhen, China). 3-Aminopropanesilicane (APTMS) and UA were purchased from Alfa Aesar. Fmoc-L-lysine, Fmoc-L-phenylalanine, 2,2′-azobis(2-methylpropionamidine)-dihydrochloride (AAPH), NaClO, and 30% hydrogen peroxide (H_2O_2) were purchased from Aladdin Chemistry Co. Ltd. (China). Cyt c from horse heart (MW 13000), DA, lipopolysaccharide (LPS), fluorescein isothiocyanate (FITC), cysteamine, catalase, and *S*-nitroso-*N*-acetyl-DL-penicillamine were obtained from Sigma-Aldrich. DL-Mandelic acid, AA, $NaNO_3$, $NaNO_2$, Na_2SO_3, Na_2CO_3, KOH, KH_2PO_4, $K_2HPO_4 \cdot 3H_2O$, NaCl, KCl, $CaCl_2$, $MgCl_2 \cdot 6H_2O$, $MnCl_2 \cdot 4H_2O$, $PbCl_2$, $CoCl_2 \cdot 6H_2O$, $CdCl_2 \cdot 2.5H_2O$, $NiCl_2 \cdot 6H_2O$, $ZnCl_2$, $AgNO_3$, $FeCl_2 \cdot 4H_2O$, $FeCl_3 \cdot 6H_2O$, KO_2, ethanol, and DMSO were obtained from Sinopharm Chemical Reagent Co. Ltd. $N_2Na_3O_3^+$ (Angeli's salt) was purchased from Santa Cruz Biotechnology. All the reagents were analytical grade and used as received. All the aqueous solutions were prepared with Milli-Q water (18.2 MΩ cm^{-1}). All electrochemical experiments were carried out at room temperature.

In the selectivity test, superoxide anion ($O_2^{\bullet-}$) was derived from dissolved KO_2 (10 μM) in the DMSO solution. Alkyl peroxyl radical ($ROO^{\bullet}$) was chemically generated by thermolysis of AAPH (10 μM) in air-saturated aqueous solution at 310 K. Hypochlorite anion (ClO^-) was provided by NaClO (10 μM).[31] Nitric oxide (NO) and nitroxyl (HNO) were derived from the solution of *S*-nitroso-*N*-acetyl-DL-penicillamine (10 μM) and Angeli's salt (10 μM), respectively.[32,33]

Synthesis and Characterization. Fmoc-L-lysine (72 mg), Fmoc-L-phenylalnine (76 mg), and sodium carbonate (40 mg) were mixed in 2 mL of Milli-Q water to generate a suspension. The suspension was then heated to about 333 K until a clear solution was observed, which can form Gel (denoted as Gel) after cooling to room temperature. For the further modification of electrode, 10 μL of hot solution was injected to the electrode surface and then immersed in 2 mL of 2 mM Cyt c for 24 h to form Cyt c/Gel. For TEM characterization of hydrogels, the Cyt/Gel and Gel samples were prepared by dipping a Cu grid with carbon film into the hydrogels with or without Cyt c, respectively. The samples were then kept in a lyophilizer for at least 12 h. In addition, FITC with the isothiocyanate group was used to conjugate with the amine group of Cyt c as a fluorescent label. In the experiment, FITC was dissolved in DMSO and then incubated with Cyt c in the dark at 277 K for 8 h. The free FITC was completely dialyzed by a semipermeable membrane for 24 h (changing the water every 8 h). The FITC conjugated with Cyt c was denoted as Cyt c/FITC. Then, Gel was immersed in Cyt c/FITC at 277 K for 1 h and denoted as Cyt c/FITC/Gel. For the control experiment, an excessive amount of cysteamine was slowly added into 50 μL of FITC and incubated in the dark at 277 K for 8 h in order to protect the amino group of gel from the isothiocyanate. Then, the products were immersed into Gel at 277 K for 1 h, to form FITC/Gel. The fluorescence images of gels were obtained by a Olympus Fluoview 1000 confocal laser, and the magnification is 20 times. Using an excitation wavelength at 488 nm, the images

dx.doi.org/10.1021/ac500231e | *Anal. Chem.* 2014, 86, 4395−4401

of FITC channel were obtained with a detection wavelength in the 525 nm.

Modification of Electrodes. An indium tin oxide (ITO)-coated glass plate was thoroughly cleaned by 1 h sonication in the following solvents: soapy water, neat ethanol, and 1 M KOH, followed by a rinse with Milli-Q water. The ITO substrate was then dried with nitrogen gas and immersed in APTMS (5% V/V) ethanol solution. Afterward, the hot solution described above at 300−310 K was injected onto an electrode for about 0.5 h. As shown in Scheme 1, the gel was then attached onto ITO substrate surface with subsequent cooling to room temperature for about 4 h, which was denoted as Gel/ITO electrode. Finally, the Gel/ITO electrode was immersed in the 2 mL solution of 0.2 mM Cyt c, FITC (previously treated with cysteamine), and Cyt c/FITC at 277 K for 1 h. The electrode was stored in a refrigerator before the electrochemical measurements and denoted as Cyt/Gel/ITO, FITC/Gel/ITO, and Cyt c/FITC/Gel/ITO electrode, respectively, which will be used hereafter. The thickness of the Gel on ITO electrode was estimated to be ~110 ± 22.8 μm.

Instruments and Measurements. An optical absorption spectrum was carried out on an Agilent 8453 UV−vis spectrometer using a quartz cuvette having 1 cm path length. A TEM image was obtained on a Hitachi S-3400N transmission electron microscope. A confocal laser scanning image was obtained with a Confocal Laser Scanning Biological Microscope (Fluoview 1000, Olympus, Japan). All rheological experiments were performed using a Thermo Scientific HAAKE RheoStress 6000 rheometer. CHI 832 electrochemical workstations (CH Instruments) were employed in all electrochemical measurements with a three-electrode electrochemical cell. The reference electrode was a KCl-saturated AglAgCl electrode, while the auxiliary electrode was a platinum wire.

Cell Cultures and Detection Released from Live Cells. Hep G2 cells were cultured in Dulbecco's Modified Eagle's medium (DMEM) containing high glucose supplemented with 10% fetal bovine serum, 100 units mL^{-1} penicillin, and 100 μg mL^{-1} streptomycin. In the proliferative period, cells (~3×10^5 cell/mL) were dispersed within replicate 96-well microliter plates to a total volume of 100 μL/well and maintained at 310 K in a 5% CO_2/95% air incubator for 24 h. Then, the Hep G2 cells were centrifuged to obtain a cell-packed pellet ($1.0-1.5 \times 10^5$ cells cm^{-2}) for the electrochemical experiments. Real sample measurements were performed in PBS containing 100 mM glucose. The device was viewed under a microscope.

RESULTS AND DISCUSSION

Characterization of Cyt c Immobilized in the Molecular Hydrogel. Figure 1A shows the processes of typical addition of Cyt c into the as-prepared molecular hydrogel (Gel). We can clearly see that the Cyt c with red color gradually penetrated into hydrogel with the increasing time from 0 to 24 h (Figure 1A, 1−5). This kind of hydrogel containing Cyt c was denoted as Cyt c/Gel. TEM images in Figure 1B,C indicate that Cyt c molecules mainly locate at the cross-link sites of the nanofibers. As a result, the aggregated Cyt c molecules reduce the density of cross-link in Gel and shorten the peptides nanofibers (~15 nm in diameter). This observation is in a good agreement with the rheological data given in Figure 2A. Frequency dependence of the modulus for Gel and Cyt c/Gel was tested by a rheological method to confirm the elastic nature of hydrogel with and without Cyt c. The dynamic storage modulus (G') is greater than the loss

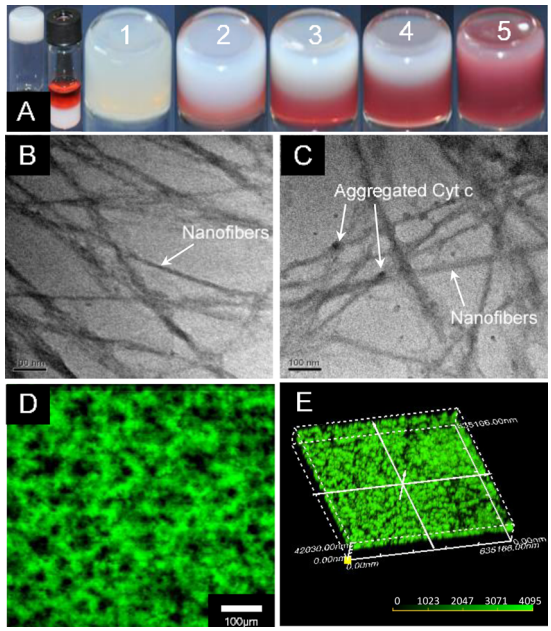

Figure 1. (A) Typical addition of 2 mM Cyt c into the as-prepared molecular hydrogel for 0, 1, 6, 12, 24 h (1−5), respectively; (B and C) TEM images of Gel (B) and Cyt c/Gel (C); (D and E) Confocal microscopic images of Cyt c/FITC/Gel film.

modulus (G''), confirming the situation of gel. The G' of Cyt c/Gel is much lower than that of Gel, suggesting that the interaction of Cyt c with the nanofibers in molecular hydrogel decreases the density of the cross-link.

Furthermore, confocal microscopy was employed to confirm whether Cyt c was immobilized in the molecular hydrogel. First of all, FITC with the isothiocyanate group was conjugated with the amino group of Cyt c and used as the fluorescence label. From the fluorescent images shown in Figure 1D,E, particularly the 3D image, we can clearly see that Cyt c was stably immobilized in the hydrogel and mainly located at the cross-link sites of the nanofibers, which agrees with the rheological and TEM data. For the comparison, the control confocal microscopic images for bare Gel and FITC/Gel, together with the electrochemical responses obtained at the different electrodes were also given in the Supporting Information (Figure S1). No fluorescence was observed for bare Gel, and the fluorescent image for FITC/Gel was completely different from that obtained for Cyt c/Gel, indicating the fluorescent images observed in Figure 1D,E are ascribed to the immobilization of Cyt c in the hydrogel. The electrochemical responses demonstrated in Figure S1D, Supporting Information, also support this conclusion. The redox reaction was only clearly observed at Cyt c/Gel/ITO electrode, while no electrochemical responses were obtained at Gel/ITO and FITC/Gel/ITO electrodes. The electrochemical investigation will be discussed in detail later.

Next, it is desirable to clarify whether Cyt c retains its inherent enzymatic activity after being immobilized in the hydrogel. The Soret band of heme protein is usually used as an indicator of the microenvironment where the heme center is located. The peak is diminished when the protein is denaturated.[34] Figure 2B depicts the UV−vis absorption spectra of (a) 0.2 mM Cyt c solution and (b) Cyt c/Gel/ITO electrode. The peak located at 409 nm corresponds to the native Cyt c solution, showing the Soret band resulting from

dx.doi.org/10.1021/ac500231e | Anal. Chem. 2014, 86, 4395−4401

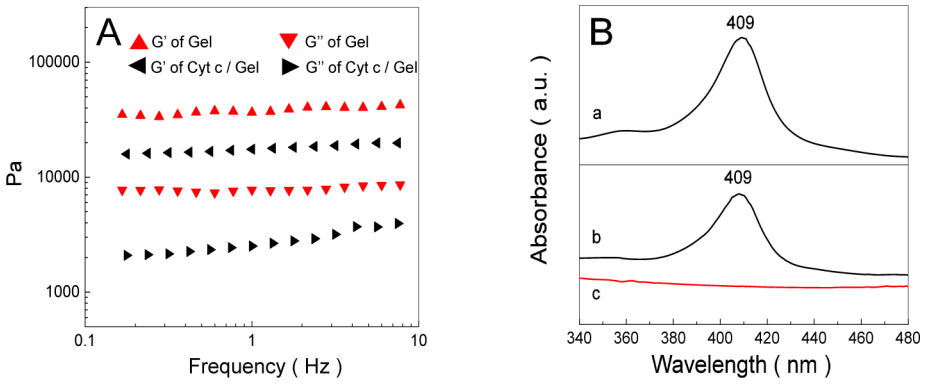

Figure 2. (A) Frequency dependence of the dynamic storage modulus (G'') and the loss modulus (G') of Gel (red) and Cyt c/Gel (black) at a strain of 2%. (B) UV−visible absorbance spectrum of (a) 0.2 mM Cyt c in Milli-Q water, (b) Cyt c/Gel/ITO electrode, and (c) Gel/ITO electrode.

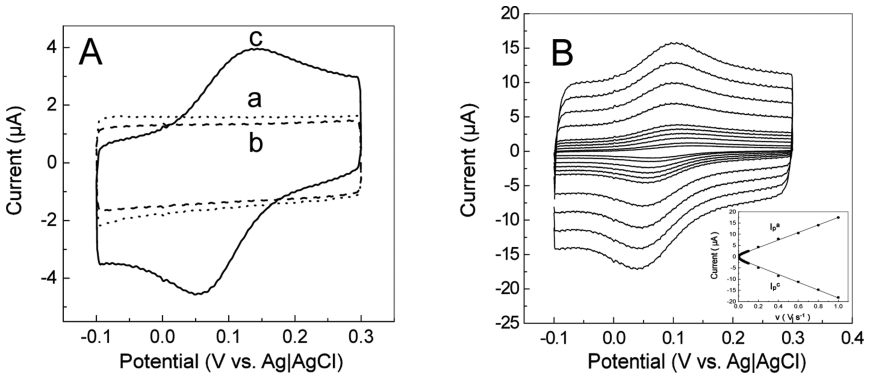

Figure 3. (A) CVs obtained at (a) bare ITO, (b) Gel/ITO, and (c) Cyt c/Gel/ITO electrodes in 10 mM PBS (pH 7.4) at scan rate of 50 mV s^{-1}. (B) CVs obtained at Cyt c/Gel/ITO electrode in 10 mM PBS (pH 7.4) at different scan rates of 10, 20, 40, 60, 80, 100, 200, 300, 400, and 500 mV s^{-1} (from inner to the outer). The inset shows the relationship between peak current and scan rate.

the $\pi-\pi^*$ transition of the porphyrin ring in Cyt c. No changes were observed in UV−vis spectrum for Cyt c/Gel/ITO electrode, implying that Cyt c processed its intrinsic activity toward H_2O_2 after being immobilized in Gel/ITO electrode, which is very beneficial for the construction of biosensor for H_2O_2.

Direct Electron Transfer of Cyt c in the Molecular Gel. As shown in Figure 3A, typical cyclic votammograms (CVs) were obtained at (a) bare ITO, (b) Gel/ITO, and (c) Cyt c/Gel/ITO electrodes in 10 mM PBS (pH 7.4). A pair of well-defined redox peaks was observed at the (c) Cyt c/Gel/ITO electrode, while only charge currents were observed at bare ITO and Gel/ITO electrodes, demonstrating that direct electron transfer of Cyt c was realized in the molecular hydrogels. The formal potential ($E^{0\prime} = (E_{p,a} + E_{p,c})/2$) of Cyt c immobilized in the Gel/ITO electrode was estimated to be 100.7 ± 3.2 mV (n = 4) versus Ag|AgCl, which is similar to those obtained at other electrode surfaces including TiO_2 nanoneedles, ZnO nanosheets, and CoOx nanoparticles.[13,14,35]

The redox reactions of Cyt c in the molecular hydrogels obtained at different scan rates in 10 mM PBS (pH 7.4) were demonstrated in Figure 3B. Both anodic and cathodic peak currents (I_p^a and I_p^c) varied linearly with potential scan rate (ν) in the range of 10−500 mV s^{-1} (inset in Figure 3B), suggesting the redox reaction is the surface-confined process. More interestingly, Cyt c/Gel/ITO electrode showed no obvious change (<3.75%) after being scanned for 1000 cycles at scan rate of 100 mV s^{-1} in 10 mM PBS (pH 7.4) (Figure S2, Supporting Information). This means that Cyt c was stably immobilized in the Gel/ITO electrode. The peak width at half peak height ($\Delta E_{p,1/2}$) was calculated to be 91.3 ± 3.5 mV (n = 4) versus Ag|AgCl at the scan rate of 10 mV s^{-1}. According to Laviron's equation, the kinetics of heterogeneous electron transfer rate constant (k_s) was estimated to be 18.36 ± 2.3 s^{-1}. This value is 1 order of magnitude greater than those obtained at gold nanostructures, TiO_2 nanotubes, and other metal oxides surfaces, such as SnO_2, WO_3, ITO, and SiO_2 surfaces, and higher than that reported at TiO_2 nanoneedles, implying that molecular hydrogel can greatly facilitate the electron transfer of proteins.[13,17,36−40]

For comparison, typical CVs were also obtained at bare ITO in (a) 10 mM PBS (pH 7.4) and (b) in 50 μM Cyt c solution and (c) after being immersed in 50 μM Cyt c solution for 0.5 h and then transferred into 10 mM fresh PBS (pH 7.4) at a scan rate of 100 mV s^{-1} (Figure S3, Supporting Information). From this figure, a pair of well-defined redox peaks was observed at bare ITO in 50 μM Cyt c solution. The formal potential at bare ITO electrode was estimated to be 99.0 ± 4.6 mV versus Ag|AgCl, which is similar to that obtained at Cyt c/Gel/ITO electrode (100.7 ± 3.2 mV). However, after being immersed in the 50 μM Cyt c solution for 0.5 h, it was found that the redox peaks dramatically decreased and little peaks remained as shown in curve c in Figure S3, Supporting Information. This demonstrates that Cyt c cannot be stably immobilized at bare ITO, compared with that in Gel.

The surface coverage amount (Γ) of electroactive Cyt c immobilized in Gel was estimated to be 1.14×10^{-10} mol cm^{-2}, based on the equation $\Gamma = Q/nFA$, in which n is the number of

dx.doi.org/10.1021/ac500231e | Anal. Chem. 2014, 86, 4395−4401

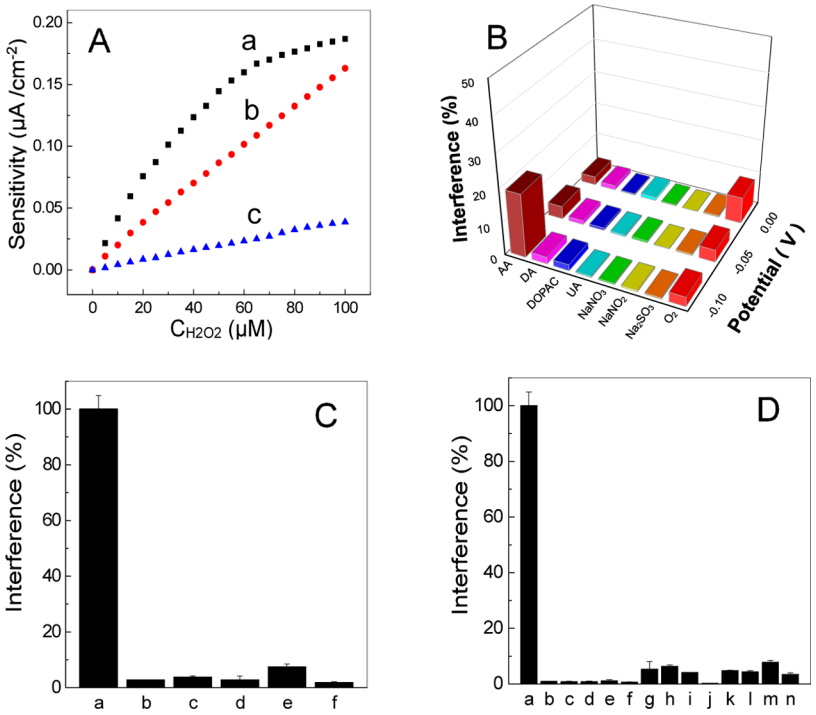

Figure 4. (A) Calibration curves of the H_2O_2 biosensor obtained at different applied potentials: (a) −0.1, (b) −0.05, (c) 0 V versus AgIAgCl in 10 mM PBS (pH 7.4). (B) The typical selectivity profile of the present biosensor obtained at different applied potentials: −0.10, −0.05, 0 V versus AgIAgCl. (C) ROS selectivity obtained at −0.05 V versus AgIAgCl toward the addition of (a) H_2O_2, (b) $O_2^{\bullet-}$, (c) $ROO^{\bullet}$, (d) ClO^-, (e) NO, and (f) HNO (10 μM for a to f). (D) Metal ion selectivity obtained at −0.05 V versus AgIAgCl toward the addition of (a) H_2O_2, (b) Na^+, (c) K^+, (d) Ca^{2+}, (e) Mg^{2+}, (f) Mn^{2+}, (g) Pb^{2+}, (h) Co^{2+}, (i) Cd^{2+}, (j) Ni^{2+}, (k) Zn^{2+}, (l) Ag^+, (m) Fe^{2+}, and (n) Fe^{3+} (10 μM for a to n).

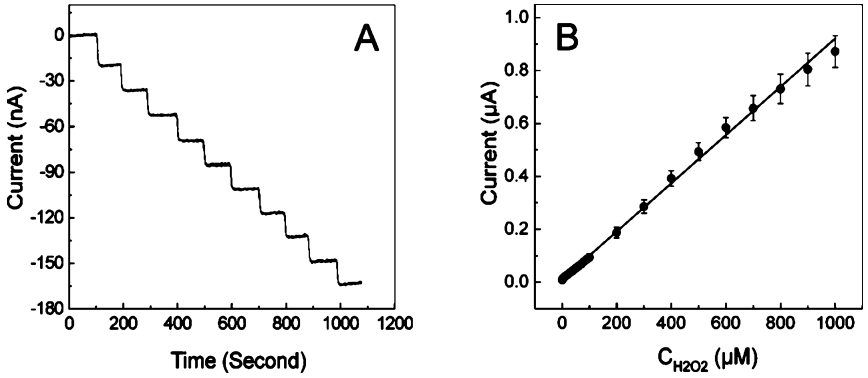

Figure 5. (A) Typical amperometric responses of Cyt c/Gel/ITO electrode to successive additions of 10 μM H_2O_2 at applied potentials of −0.05 V versus AgIAgCl in 10 mM PBS (pH 7.4). (B) The calibration plot of steady-state currents against concentrations of H_2O_2.

electrons transferred, F is Faraday's constant, and A is the electrode surface area (~0.7 cm^2). This value is greater than that of the monolayer, which was reported to be ~2.41 × 10^{-12}.[41] Meanwhile, this surface coverage amount is comparable with that of the multilayer.[42] As a matter of fact, stable Cyt c multilayers were constructed, in which Cyt c can effectively exchange electrons with the electrode without the need of a mediator.[42]

Analytical Performance of Gel-Immobilized Cyt c for H_2O_2. The electron transfer of Cyt c was facilitated at the Gel/ITO surface, and the enzyme activity of Cyt c was also maintained in the molecular hydrogel as demonstrated above. Thus, the data provided an approach for constructing the third-generation biosensor for H_2O_2 because the heme has been well documented as the active site for the catalysis of the reduction of H_2O_2. As a matter of fact, the sensitivity and selectivity of electrochemical biosensors are dependent on the applied potentials. As shown in Figure 4A, sensitivity of the present Cyt c/Gel/ITO H_2O_2 biosensor increased with the negative shift of the applied potentials; namely, the more negative the applied potential, the higher was the sensitivity of the biosensor.

Meanwhile, selectivity of electrochemical biosensors is also potential dependent. Figure 4B shows eight kinds of potential interferences under different applied potentials. At the negative potential, e.g., −0.1 V, the present H_2O_2 biosensor was free from anodic interferences like AA, UA, DA, DOPAC, NO_2^-, NO_3^-, and SO_3^{2-}, but 8% of cathodic response current from 200 μM O_2 was observed relative to 100 μM H_2O_2. On the other hand, at the more positive potential, e.g., 0 V, 22.1% of anodic current of 100 μM AA was obtained relative to 100 μM H_2O_2. Fortunately, at the suitable potential of −0.05 V, both

dx.doi.org/10.1021/ac500231e | Anal. Chem. 2014, 86, 4395−4401

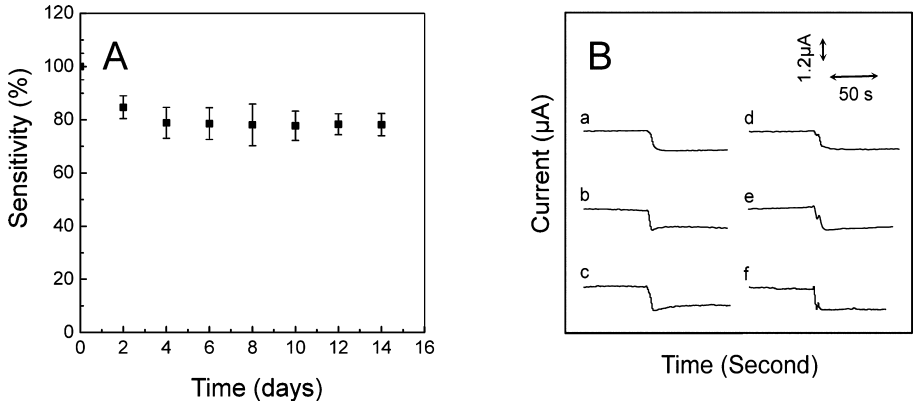

Figure 6. (A) Stability test for Cyt c/Gel/ITO electrode at −0.05 V versus AglAgCl in 10 mM PBS (pH 7.4) over 2 weeks. (B) Reproducibility test for the Cyt c/Gel/ITO electrode monitored over 6 different sensors (from a to f) with the addition of 10 μM H_2O_2 at −0.05 V versus AglAgCl in 10 mM PBS (pH 7.4).

anodic and cathodic potential interferences were negligible. Therefore, for fulfilling both the selectivity and sensitivity of the present biosensor, −0.05 V (vs AglAgCl) was selected as the working potential. In addition, the selectivity of the present H_2O_2 over reactive oxygen species (ROS) and metal ions was also examined. As demonstrated in Figure 4C,D, negligible interferences were observed for other typical ROS including $O_2^{\bullet -}$, $ROO^{\bullet}$, ClO^-, NO, HNO, and metal ions with 100-fold concentration compared with that of H_2O_2. These results demonstrated that the present Cyt c/Gel/ITO electrode showed high selectivity for H_2O_2 over typical ROS, metal ions, O_2, and other biological species at the working potential of −0.05 V vs AglAgCl.

Amperometric responses of Cyt c/Gel/ITO electrode on successive addition of 10 μM H_2O_2 were obtained in 10 mM PBS (pH 7.4) at the applied potential of −0.05 V. No response was observed at the bare ITO and Gel/ITO surfaces, while well-defined steady-state current responses were obtained and the currents increased stepwise with successive additions of H_2O_2, as given in Figure 5A. The response time of the present biosensor for H_2O_2 was observed to be less than 6 s. The calibration plot of steady-state currents against concentrations of H_2O_2 is given in Figure 5B. The dynamic detection linear range for H_2O_2 was estimated to be $\sim 3 \times 10^{-7}$ to $\sim 8 \times 10^{-4}$ M with a detection limit of 50 nM (S/N = 3:1). Compared with other H_2O_2 biosensors based on gels reported so far (Table S1, Supporting Information), besides higher selectivity, the present H_2O_2 biosensor exhibits wider linear detection range and lower detection limit.[40,43,44] The high selectivity and sensitivity, together with broad dynamic range and low detection limit, fulfill the requirement of real time tracking of H_2O_2 concentration in a biological system.

In addition, the 3D network of molecular hydrogel enables Cyt c immobilized in it to show good stability. As shown in Figure 6A, the response current for H_2O_2 was recorded three times daily, and the current responses just decreased <5% at the first 3 days and had almost no changes over 2 weeks, indicating the long-term stability of the present biosensor. Moreover, as demonstrated in Figure 6B, the deviation of the current responses of 6 sensors prepared with the same method did not exceed 6.2% (RSD).

Determination of H_2O_2 Released from Live Cells. As demonstrated above, the present biosensor for H_2O_2 with high analytical performance, as well as the specific characteristic of hydrogels such as good biocompatibility and water-solubility, provided a platform for real time monitoring of H_2O_2 released from live cells. Typical amperometric responses of Cyt c/Gel/ITO electrode, which was located near Hep G2 cell lines, were obtained at applied potentials of −0.05 V versus AglAgCl in 10 mM PBS (pH 7.4) after the injection of 5 μg mL^{-1} LPS and 250 U mL^{-1} catalase. As shown in Figure 7, the cathodic

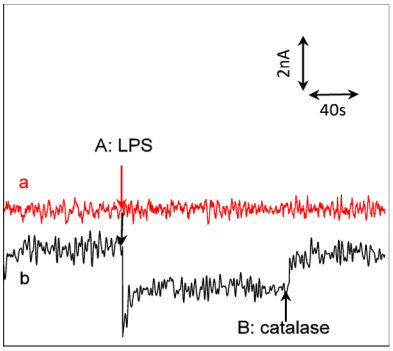

Figure 7. Amperometric responses obtained at the (a) bare Gel/ITO and (b) Cyt c/Gel/ITO electrodes located near Hep G2 cells at applied potentials of −0.05 V versus AglAgCl in 10 mM PBS (pH 7.4) with the addition of (A) 5 μg mL^{-1} LPS and (B) 250 U mL^{-1} catalase.

current gradually increased at Cyt c/Gel/ITO electrode with the addition of LPS (curve b), which was reported to generate H_2O_2 from live cells.[45] Then, the system was slowly stirred, and the reduction current of ~1.9 nA was observed in 70 s, while no response was obtained at bare Gel/ITO electrode with the same addition of LPS (curve a). Furthermore, after 250 U mL^{-1} catalase was injected, a selective scavenger of H_2O_2, into the solution, the current shown in curve b decreased rapidly and went almost down to the background. Therefore, it can be concluded that the increased cathodic current observed in curve b is attributed to the enzymatic reduction of H_2O_2, which is effectively mediated by the Cyt c immobilized in the molecular hydrogels.

CONCLUSIONS

In summary, we have developed a third generation biosensor for H_2O_2 based on molecular hydrogel-stabilized Cyt c, in which electron transfer of Cyt c is greatly enhanced in the molecular hydrogel. Meanwhile, Cyt c has maintained its bioactive activity after being immobilized in the hydrogel, thus

dx.doi.org/10.1021/ac500231e | Anal. Chem. 2014, 86, 4395−4401

providing a direct platform for determination of H_2O_2. The present biosensor shows high selectivity against other ROS, metal ions, oxygen, and other biological species, as well as broad linear range and low detection limit. Furthermore, the hydrogel-immobilized enzyme electrode exhibits long-term stability and good reproducibility. Accordingly, the present biosensor has been successfully applied in determination of H_2O_2 released from live cells. This work has paved a new way to understanding the role that ROS plays in the biological and pathological systems. This methodology can be extended to design and develop the biosensors for other ROS, metal ions, proteins, and so on, based on small molecular hydrogels.

■ ASSOCIATED CONTENT

Supporting Information

Confocal fluorescence images and electrochemical responses for Cyt c/Gel, FITC/Gel, and Cyt c/FITC/Gel films; stability test for CVs; electrochemical responses for bare ITO in PBS and PBS containing Cyt c and ITO immersed in Cyt and then transferred into fresh PBS; comparison for analytical performance. This material is available free of charge via the Internet at http://pubs.acs.org.

■ AUTHOR INFORMATION

Corresponding Authors

*E-mail: yangtian@tongji.edu.cn. Fax: 0086-21-65981097.
*E-mail: qgwang66@tongji.edu.cn. Fax: 0086-21-65981097.

Notes

The authors declare no competing financial interest.

■ ACKNOWLEDGMENTS

This research was supported by the National Natural Science Foundation of China (21175098, 21274111, and 21305104) and National Natural Science Fund for distinguished young scholars (21325521).

■ REFERENCES

(1) Wooten, M.; Karra, S.; Zhang, M.; Gorski, W. *Anal. Chem.* **2014**, *86*, 752−757.
(2) Shleev, S.; Tkac, J.; Christenson, A.; Ruzgas, T.; Yaropolov, A. I.; Whittaker, J. W.; Gorton, L. *Biosens. Bioelectron.* **2005**, *20*, 2517−2554.
(3) Gill, R.; Zayats, M.; Willner, I. *Angew. Chem., Int. Ed.* **2008**, *47*, 7602−7625.
(4) (a) Tatsuma, T.; Watanabe, T. *Anal. Chem.* **1991**, *63*, 1580−1585. (b) Tatsuma, T.; Watanabe, T.; Tatsuma, S.; Watanabe, T. *Anal. Chem.* **1994**, *66*, 290−294. (c) Komori, K.; Takada, K.; Tatsuma, T. *Langmuir* **2006**, *22*, 478−483.
(5) (a) Su, T. J.; Lu, J. R.; Thomas, R. K.; Cui, Z. F.; Penfold, J. *Langmuir* **1998**, *14*, 438−445. (b) Murgida, D. H.; Hildebrandt, P. *Phys. Chem. Chem. Phys.* **2005**, *7*, 3773−3784.
(6) Willner, B.; Katz, E.; Willner, I. *Curr. Opin. Biotechnol.* **2006**, *17*, 589−596.
(7) Leger, C.; Bertrand, P. *Chem. Rev.* **2008**, *108*, 2379−2438.
(8) Eddowes, M. J.; Hill, H. A. O. *J. Am. Chem. Soc.* **1979**, *101*, 4461−4464.
(9) Reed, D. E.; Hawkridge, F. M. *Anal. Chem.* **1907**, *59*, 2334−2339.
(10) Haymond, S.; Babcock, G. T.; Swain, G. M. *J. Am. Chem. Soc.* **2002**, *124*, 10634−10635.
(11) Wu, J. F.; Xu, M. Q.; Zhao, G. C. *Electrochem. Commun.* **2010**, *12*, 175−177.
(12) Zhu, A. W.; Tian, Y.; Liu, H. Q.; Luo, Y. P. *Biomaterials* **2009**, *30*, 3183−3188.
(13) Luo, Y. P.; Liu, H. Q.; Rui, Q.; Tian, Y. *Anal. Chem.* **2009**, *81*, 3035−3041.
(14) Rui, Q.; Komori, K.; Tian, Y.; Liu, H. Q.; Luo, Y. P.; Sakai, Y. *Anal. Chim. Acta* **2010**, *670*, 57−62.
(15) Li, X. G.; Liu, Y.; Zhu, A. W.; Luo, Y. P.; Deng, Z. F.; Tian, Y. *Anal. Chem.* **2010**, *82*, 6512−6518.
(16) Zhu, A. W.; Luo, Y. P.; Tian, Y. *Anal. Chem.* **2009**, *81*, 7243−7247.
(17) Liu, H. Q.; Tian, Y.; Deng, Z. F. *Langmuir* **2007**, *23*, 9487−9494.
(18) Oommen, O. P.; Wang, S.; Kisiel1, M.; Sloff, M.; Hilborn, J.; Varghese, O. P. *Adv. Funct. Mater.* **2013**, *23*, 1273−1280.
(19) Yang, Z.; Liang, G.; Xu, B. *Acc. Chem. Res.* **2008**, *41*, 315−326.
(20) Yang, Z.; Xu, K.; Wang, L.; Gu, H.; Wei, H.; Zhang, M.; Xu, B. *Chem. Commun.* **2005**, *35*, 4414−4416.
(21) Toledano, S.; Williams, R. J.; Jayawarna, V.; Ulijn, R. V. *J. Am. Chem. Soc.* **2006**, *128*, 1070−1071.
(22) Kiyonaka, S.; Sada, K.; Yoshimura, I.; Shinkai, S.; Kato, N.; Hamachi, I. *Nat. Mater.* **2004**, *3*, 58−64.
(23) Wang, Q. G.; Yang, Z. M.; Wang, L.; Ma, M.; Xu, B. *Chem. Commun.* **2007**, 1032−1034.
(24) Wang, Q. G.; Yang, Z. M.; Zhang, X. Q.; Xiao, X. D.; Chang, C. K.; Xu, B. *Angew. Chem., Int. Ed.* **2007**, *46*, 4285−4289.
(25) Guiseppi-Elie, A. *Biomaterials* **2010**, *31*, 2701−2716.
(26) Wang, Z.; Liu, S.; Wu, P.; Cai, C. *Anal. Chem.* **2009**, *81*, 1638−1645.
(27) Michael, H. F.; Jackson, R. H.; Michael, C. L. *Anal. Chem.* **2013**, *85*, 4057−4065.
(28) Forzani, E. S.; Zhang, H.; Nagahara, L. A.; Amlani, I.; Tsui, R.; Tao, N. *Nano Lett.* **2004**, *9*, 1785−1788.
(29) Moreno-Castilla, C.; Maldonado-Hodar, F. J. *Carbon* **2005**, *43*, 455−465.
(30) Florence, T. M. *J. Inorg. Biochem.* **1985**, *23*, 131−141.
(31) Li, L.; Zhu, A. W.; Tian, Y. *Chem. Commun.* **2013**, *49*, 1279−1281.
(32) Singh, R. J.; Hogg, N.; Joseph, J.; Kalyanaraman, B. *J. Biol. Chem.* **1996**, *271*, 18596−18603.
(33) Solomon, S. B.; Bellacia, L.; Sweeney, D.; Piknova, B.; Perlegas, A.; Helms, C. C.; Ferreyra, G. A.; King, S. B.; Raat, N. J. H.; Kern, S. J.; Sun, J.; McPhail, L. C.; Schechter, A. N.; Natanson, C.; Gladwin, M. T.; Kim-Shapiro, D. B. *Free Radical Biol. Med.* **2012**, *53*, 2229−2239.
(34) Wang, S. F.; Chen, T.; Zhang, Z. L.; Shen, X. C.; Lu, Z. X.; Pang, D. W.; Wong, K. Y. *Langmuir* **2005**, *21*, 9260−9266.
(35) Mohammadi, A.; Moghaddam, A. B. *Micro. Nano Lett.* **2012**, *7*, 951−954.
(36) Sarauli, D.; Riedel, M.; Wettstein, C.; Hahn, R.; Stiba, K.; Wollenberger, U.; Leimkuhler, S.; Schmuki, P.; Lisdat, F. *J. Mater. Chem.* **2012**, *22*, 4615−4618.
(37) Nasr, C.; Hotchandani, S. *Chem. Mater.* **2000**, *12*, 1529−1535.
(38) Deng, Z. F.; Gong, Y.; Luo, Y. P.; Tian, Y. *Biosens. Bioelectron.* **2009**, *24*, 2465−2469.
(39) Shi, G.; Sun, Z.; Liu, M.; Zhang, L.; Liu, Y.; Qu, Y.; Jin, L. *Anal. Chem.* **2007**, *79*, 3581−3588.
(40) Wang, Y.; Bian, X.; Liao, L.; Zhu, J.; Guo, K.; Kong, J.; Liu, B. *Microchim. Acta* **2012**, *178*, 277−283.
(41) Shie, J. W.; Yogeswaran, U.; Chen, S. M. *Talanta* **2008**, *74*, 1659−1669.
(42) Beissenhirtz, M. K.; Scheller, F. W.; Stocklein, W. F. M.; Kurth, D. G.; Mohwald, H.; Lisdat, F. *Angew. Chem., Int. Ed.* **2004**, *43*, 4357−4360.
(43) Hu, J.; Yu, Y.; Guo, H.; Chen, Z.; Li, A.; Feng, X.; Xi, B.; Hu, G. *J. Mater. Chem.* **2011**, *21*, 5352−5359.
(44) Liu, C. Y.; Hu, J. M. *Biosens. Bioelectron.* **2009**, *24*, 2149−2154.
(45) Kono, K.; Salazar-Onfray, F.; Petersson, M.; Hansson, J.; Masucci, G.; Wasserman, K.; Nakazawa, T.; Anderson, P.; Kiessling, R. *Eur. J. Immunol.* **1996**, *26*, 1308−1313.